Rapid Report

A residue in the intracellular vestibule of the pore is critical for gating and permeation in Ca^{2+}-activated K^+ (BK_{Ca}) channels

J. D. Lippiat, N. B. Standen and N. W. Davies

Ion Channel Group, Department of Cell Physiology and Pharmacology, University of Leicester, PO Box 138, Leicester LE1 9HN, UK

(Received 13 July 2000; accepted after revision 27 September 2000)

1. We have used patch clamp to record large-conductance Ca^{2+}-activated K^+ (BK_{Ca}) currents from a human embryonic kidney cell line (HEK293) expressing wild-type and mutant *hSlo*α channels.

2. When we mutated F380 in the S6 region, thought to contribute to the intracellular vestibule of the pore, to isoleucine (F380I), very little channel activity was recorded. In contrast, mutation to tyrosine (F380Y) resulted in significant voltage-dependent currents.

3. The unitary conductances of F380I, F380Y and wild-type channels were 92 ± 6 pS ($n = 3$), 166 ± 5 pS ($n = 3$) and 294 ± 5 pS ($n = 5$), respectively.

4. Both mutant and wild-type *hSlo*α channels were sensitive to 100 nM iberiotoxin.

5. The F380Y mutant produced channels that were active at negative membrane potentials, even in the absence of Ca^{2+}.

6. We conclude that this conserved residue within BK_{Ca} channels may line the conduction pathway and forms a key element of the gating mechanism.

Large conductance Ca^{2+}-activated K^+ (BK_{Ca}) channels occur in many cells where they play an important role in regulating membrane excitability. Generally their activity is increased by depolarization and their voltage sensitivity is shifted to more negative values by an increase in intracellular [Ca^{2+}]. BK_{Ca} channels have a characteristically high conductance, ranging from approximately 100 pS to 250 pS depending on the ionic conditions, but they maintain a surprisingly high selectivity for K^+ (Blatz & Magleby, 1984; Lippiat *et al.* 1998). Consequently, the opening of only a few of these channels can produce a significant rise in membrane K^+ conductance. Functional BK_{Ca} channels that are both voltage and Ca^{2+} dependent are formed from a tetrameric assembly (Shen *et al.* 1994) of pore-forming α subunits which share close homology with voltage-gated K^+ (Kv) channel α subunits. They differ by having additional hydrophobic segments (S0–S10 in total) resulting in an extracellular N-terminal region and a longer intracellular C-terminal region (Meera *et al.* 1997). As with most members of the potassium channel superfamily, a GYG motif exists in the P-region between the S5 and S6 transmembrane segments which is likely to form the narrowest part of the conduction pathway and confers K^+ selectivity (Doyle *et al.* 1998). Aromatic residues located near the external mouth of the pore have been shown to affect both permeation and gating of dSlo channels (Lagrutta *et al.* 1998).

There is a highly conserved region between S9 and S10 on the C terminal region which has been termed the 'Ca^{2+} bowl'. Mutations of important aspartate residues in this region decrease the Ca^{2+} sensitivity but not the Cd^{2+} sensitivity of BK_{Ca} channels, suggesting the existence of other divalent ion binding sites (Schreiber & Salkoff, 1997). Kinetic studies of native and cloned BK_{Ca} channels suggest that several sites interact with Ca^{2+} with varying degrees of cooperativity (McManus & Magleby, 1991; DiChiara & Reinhardt, 1995). It is not known how binding of calcium ultimately results in increased open probability. Molecular separation of Slo α into the Kv-like S0–S8 'core' and the S9–S10 'tail' and their subsequent co-expression yields functional channels identical to wild-type channels; however, expression of either the core or tail alone results in non-functional channels (Wei *et al.* 1994). Furthermore, experiments done on chimeras between mSlo1 and a related but Ca^{2+}-independent channel, mSlo3, indicate that inhibition of channel opening is produced by association of the tail and core, and that this inhibition is relieved by intracellular Ca^{2+} (Schreiber *et al.* 1999).

In this paper, we describe experiments done on wild-type *hSloα* channels and on channels containing two mutations of residue F380 within membrane spanning domain S6. These mutants were F380I, which is the equivalent residue in the Kv channels *Shaker*, hKv1.1 and hDRK1, and F380Y, the equivalent residue in herg (Fig. 1). Both mutations reduced single channel conductance. We found also that residue F380 has a critical role in determining the activation kinetics of *hSloα* channels. The conservative mutation to tyrosine (F380Y) caused a dramatic change in the voltage- and Ca^{2+}-dependent activation of the channel, resulting in a substantial open probability even in the absence of Ca^{2+}. The effect of mutating this residue on the relationship between channel activation, Ca^{2+} and voltage is quantitatively greater than those of mutations made within the 'Ca^{2+} bowl' (see Fig. 1*A*), a Ca^{2+}-binding region in the S9–S10 linker (Schreiber & Salkoff, 1997).

METHODS

Molecular biology and cell culture

The expression construct pcDNA6-*hSloα* was generated and donated by Dr Peter Stacey (Pfizer Central Research, Sandwich, Kent, UK). The insert had an amino acid sequence with complete identity to GenBank entry U23767; the amino acid positions noted in this paper correspond to this clone (see Fig. 1). The cDNA was mutated by the QuikChange (Stratagene) method which involved amplification by PCR of the entire construct using forward and reverse primers that both contained the desired DNA sequence in the region of interest. The wild-type DNA that served as the template in the PCR reaction was digested by *Dpn* I which cuts GmATC. Transformation of XL1-Blue supercompetent cells with the products of the reactions yielded colonies that grew on ampicillin-containing (100 μg ml^{-1}) LB-agar, of which a few were screened for *hSloα* mutants by sequencing. All constructs used in this study had the entire *hSloα* insert sequenced to ensure no further mutations had arisen as a result of the PCR reactions. Quality-controlled sequencing was performed in all cases by Lark Technologies.

Human embryonic kidney cells (HEK 293 cell line; ECACC no. 85120602) were transfected with the constructs using the lipofectamine protocol (Life Technologies). The transfection mixture per 35 mm well contained 6 μl lipofectamine reagent and 1 μl DNA in 1 ml media. Clones that were maintained after 16 days exposure to the culture medium (minimal essential medium (MEM) supplemented with 10% (v/v) fetal bovine serum, 1% L-glutamine, 1% non-essential amino acids (Life Technologies), 1% sodium pyruvate (Sigma), containing 5 μg ml^{-1} blasticidin were used for this study. Non-transfected HEK cells were killed by this selective media within 14 days.

The stable lines were cultured in the selective media in an incubator set at 37°C and in an atmosphere of 95% air and 5% CO_2. For experimentation, samples of cells were plated onto 35 mm Petri dishes that had been coated with high molecular weight poly-L-lysine (Sigma), and studied over the following 1–4 days. Over the course of this study, the cell lines were subcultured 15–20 times.

Electrophysiology

Currents through BK_{Ca} channels were recorded using either the inside-out or outside-out configuration of the patch-clamp technique (Hamill *et al.* 1981). Glass micropipettes were pulled from thick-walled borosilicate capillaries (Clarke Electromedical), coated with Sylgard (Dow Corning) and polished to give resistances between 5 and 15 MΩ when filled with experimental solution. Membrane

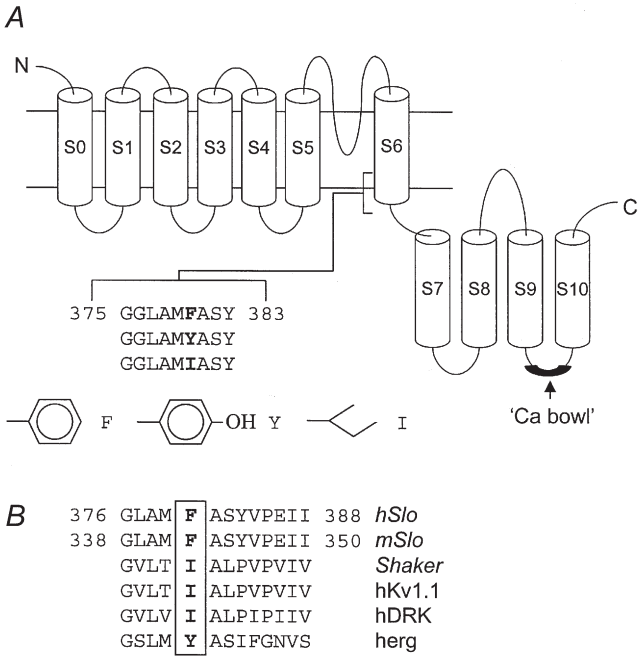

Figure 1. Diagram showing the membrane spanning regions of *hSloα* and the location of residue F380

A, residue F380 is located in the S6 domain, as indicated. This residue was mutated to either I or Y. The side chain carbon-backbone of each residue is shown below. *B*, sequence alignments of the corresponding regions of *mSlo*, *Shaker*, hKv1.1, hDRK and herg with *hSlo* (based on Doyle *et al.* 1998).

patches were placed in the outflow of a perfusion pipette which allowed changing between five different solutions bathing the patch. When necessary, vesicles associated with inside-out patches were ruptured by taking the patch out of the bath solution transiently. Currents were measured with a List EPC-7 amplifier, filtered at 3 kHz and digitized at 10 or 20 kHz with a DigiData 1200 interface (Axon Instruments). Voltage protocols and data acquisition were controlled by a computer program written using AxoBASIC routines. A *P*/6 sequence was used to subtract leak and capacity currents when appropriate. Membrane potentials are expressed conventionally as inside (of the membrane) relative to outside, and outward currents are defined as positive and plotted upwards. Experiments were done at room temperature (20–24°C).

Solutions

The extracellular solution contained 50 mM K_2SO_4, 40 mM KCl (140 mM total K^+), 1 mM $CaCl_2$, 1 mM $MgCl_2$ and 10 mM Hepes. The intracellular solutions also contained 50 mM K_2SO_4, 10 mM Hepes and KOH/KCl to give 140 mM total K^+ after adjusting the pH. To obtain intracellular Ca^{2+} concentrations of 10 μM and 1 μM, HEDTA (10 mM) was used to buffer Ca^{2+}; for lower Ca^{2+} concentrations, EDTA was used. The total Ca^{2+} to be added to give the desired free concentration was calculated using the program Maxchelator (http://www.stanford.edu/%7Epatton/maxc.html). For solutions with [Ca^{2+}] of 30 and 100 μM, the calcium chelator was replaced by 10 mM sorbitol, and total Ca^{2+} calculated according to the buffering capacity of SO_4^{2-} ions alone. The pH of each solution was adjusted to 7.2 with HCl.

Stock solutions of iberiotoxin (IbTX) were made up in water and subsequently diluted by at least 1000-fold to give the concentrations used in this study.

Analysis

Activation was measured as conductance, since the symmetrical K^+ gives a consistent unitary conductance in this range. The data points were fitted with a Boltzmann distribution, which yielded values for $V_{\frac{1}{2}}$, k and G_{max}:

$$G = \frac{G_{max}}{1 + \exp((V - V_{\frac{1}{2}})/k)}, \quad (1)$$

where $V_{\frac{1}{2}}$ is the voltage at which the conductance (G) is half the maximum conductance (G_{max}) and k is a factor affecting the steepness of the relationship. Data were normalized by dividing by the fitted maximum G_{max} for each patch. Exponential fits to current relaxations and generation of mean–variance plots were done using software developed in our laboratory; all other analysis was done using Excel (Microsoft) or SigmaPlot (SPSS).

RESULTS

Mutations of F380 alter unitary conductance and open times

BK_{Ca} currents were recorded using either inside-out or outside-out patches from HEK293 cells expressing wild-type *hSlo*α, *hSlo*αF380I or *hSlo*αF380Y channels. All the experiments were done in symmetrical 140 mM K^+ and both internal and external solution contained 50 mM SO_4^{2-} ions to chelate any contaminating Ba^{2+} ions (Miller *et al.* 1987). Cells expressing wild-type *hSlo* and the F380Y mutant channels produced currents that were usually macroscopic in isolated patches. The expression level of wild-type and F380Y channels was similar. Currents recorded from cells expressing F380I channels, however, were very much smaller and reflected the low open probability of these channels even in high Ca^{2+}. In all three cases, the currents were confirmed as flowing through BK_{Ca} channels by their sensitivity to the specific BK_{Ca} channel blocker iberiotoxin (Fig. 2). It is possible that mutating F380 alters iberiotoxin sensitivity slightly, but we have not investigated this further. Figure 2*B* shows unitary recordings from wild-type, F380I and F380Y channels. The conductance of wild-type channels was 294 $\pm$ 5 pS ($n = 5$), which is similar to values reported for other BK_{Ca} channels under these conditions (Blatz & Magleby, 1984; Wallner *et al.* 1995; Lippiat *et al.* 1998; Ottolia *et al.* 1999). The conductances of F380I and F380Y channels were 31 and 56% of the wild-type value at 92 $\pm$ 6 pS ($n = 3$) and 166 $\pm$ 5 pS ($n = 3$), respectively. Not only did mutating F380 alter single channel conductance, but it also had a profound effect on the kinetics of the channels observed. The open times of the F380I channels were much shorter than wild-type values, and it was difficult to find openings that were long enough to reach full amplitude. Because of the small amount of current obtained with F380I, we were unable to obtain accurate measurements of Ca^{2+} sensitivity or kinetic data for this mutant.

Voltage dependence is altered in F380Y channels

The voltage dependence of activation of both wild-type and the F380Y mutant channels was measured in inside-out patches exposed to a range of [Ca^{2+}]. Membrane potential was held at −80 mV and a series of test potentials ranging from −70 to +80 mV was applied. The 150 ms pulse was long enough for the evoked currents to reach steady state. Because currents were measured from isolated patches we repeated each step 10 times and the analysis was done on the average of these currents. Examples of current families for wild-type and F380Y channels at 0, 1 and 10 μM Ca^{2+} are shown in Fig. 3*A*. It is clear that in the absence of Ca^{2+}, even at quite negative potentials, there is considerable activation of F380Y channels. Note also that the deactivation time course is much slower in this mutant than in wild-type channels. The steady-state activation at different voltages was quantified by plotting the chord conductance (calculated from the reversal potential of 0 mV) against membrane potential. A Boltzmann relation (eqn (1)) was fitted to the data and individual data points for each patch were then normalized to the maximum conductance (G_{max}) returned by the fit. Activation curves obtained in this way for a range of [Ca^{2+}] are shown in Fig. 3*B*. Much less Ca^{2+} was needed to activate F380Y channels compared to that needed for wild-type channels, as illustrated by plotting $V_{1/2}$ against [Ca^{2+}] for wild-type and mutant channels (Fig. 3*C*). Another noticeable feature is that although the channel containing the F380Y mutation remained voltage dependent it was less so than the wild-type

channel; the average slope factors (k in eqn (1)) were 11.5 ± 0.4 mV ($n = 10$) and 27.0 ± 1.8 mV ($n = 18$) for wild-type and F380Y channels, respectively (combined $[Ca^{2+}]$). The enhanced activity of the F380Y mutant was also evident after constructing mean–variance plots of wild-type currents in 10 μM Ca^{2+} and F380Y currents in 'zero' Ca^{2+} (no added Ca^{2+}). Examples of mean–variance plots obtained at +80mV from wild-type (83 pulses, 10 μM Ca^{2+}) and F380Y (100 pulses, 'zero' Ca^{2+}) channels are shown in Fig. 3*D*. It can be seen that the maximum open probability (P_{open}) reached was only slightly lower for F380Y channels in 'zero' Ca^{2+} than for wild-type channels in 10 μM Ca^{2+}.

Deactivation kinetics of F380Y channels are slower than those of wild-type channels

As mentioned above, examination of the current traces of wild-type and F380Y channels revealed that the deactivation kinetics of the mutant were much slower than those of wild-type. We investigated this further by fitting both activation and deactivation time courses at a range of voltages and internal $[Ca^{2+}]$ with a single exponential function. Figure 4*A* shows examples of the fits of both wild-type and F380Y currents in 10 μM Ca^{2+}. Because of the high level of steady-state activity of F380Y channels, even at low internal $[Ca^{2+}]$ and at negative potentials, it was difficult to obtain accurate fits for this mutant at $[Ca^{2+}]$ higher than 10 μM. Plots of the fitted time constants against membrane potential at various $[Ca^{2+}]$ are shown in Fig. 4*B*. The most obvious difference is that the deactivation time constants are much slower in the mutant channel at negative membrane potentials. In the presence of Ca^{2+}, however, the time constants of wild-type and F380Y channels were similar at positive potentials. We fitted the relationships between membrane potential and time constants

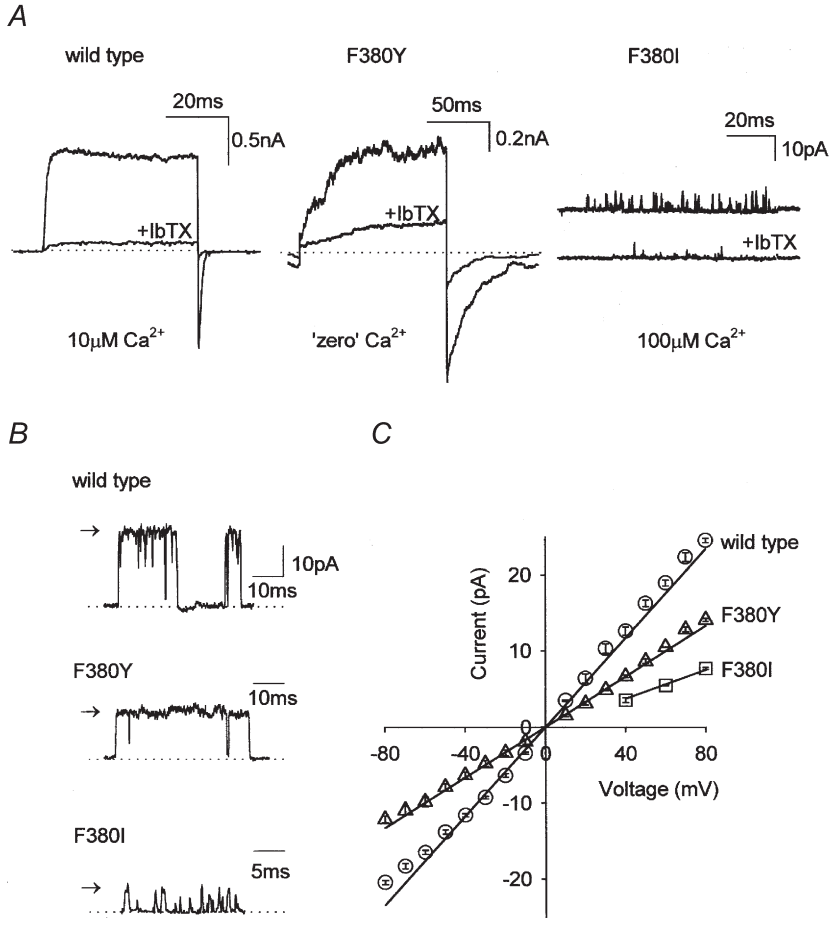

Figure 2. Currents through F380Y and F380I channels are iberiotoxin sensitive and have reduced single channel conductance compared to wild-type *hSlo*α channels

A, examples of currents elicited from wild-type, F380Y and F380I channels by voltage steps from –80 to +80 mV in outside-out patches. In all cases, the current was significantly reduced by application of 100 nM iberiotoxin (IbTX). The $[Ca^{2+}]$ in the pipette was 10 μM for wild-type, 'zero' for F380Y and 100 μM for F380I. *B*, single channel currents recorded at +80 mV for wild-type, F380Y and F380I channels, as indicated. *C*, a plot of the single channel current against membrane potential for wild-type (○, $n = 5$), F380Y (△, $n = 3$) and F380I (□, $n = 3$) channels. Error bars (S.E.M.) are within the symbols.

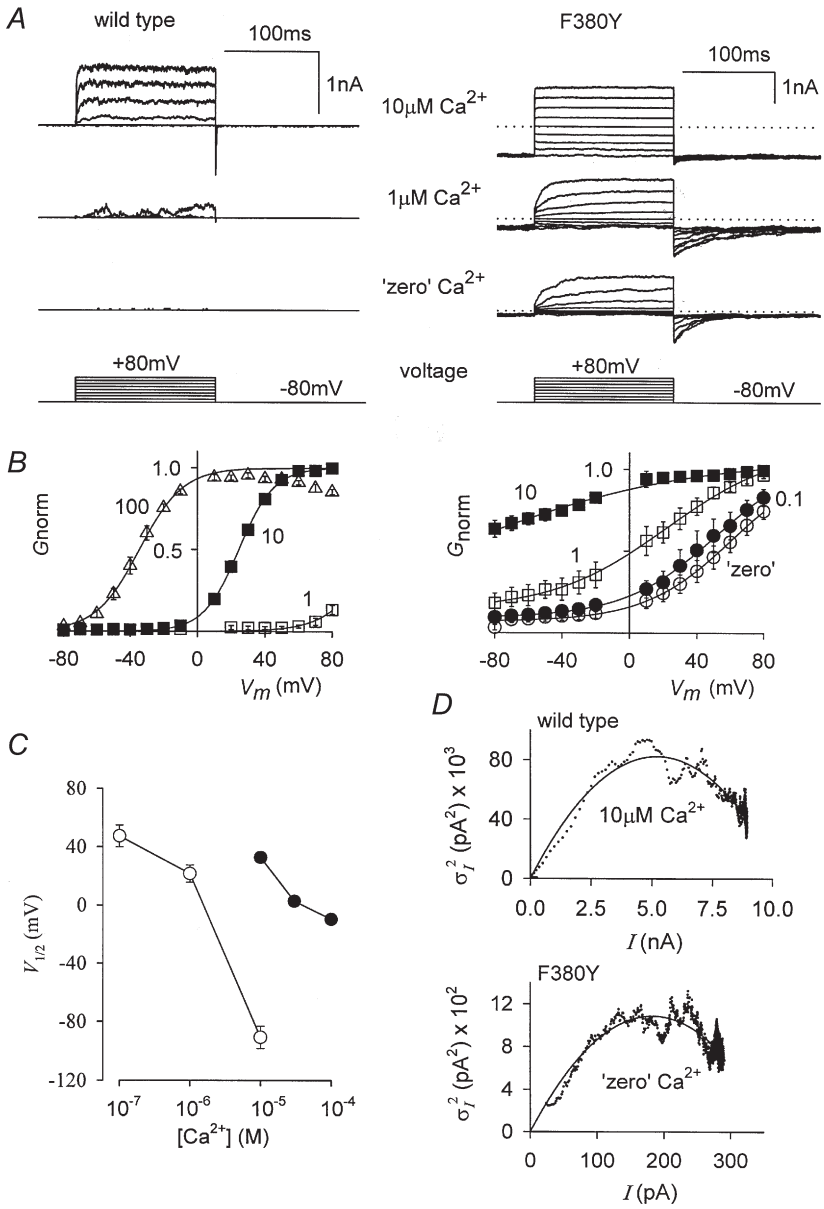

Figure 3. The voltage and Ca^{2+} sensitivity of wild-type and F380Y *hSlo*α channels are different

A, representative current families (individual records) from wild-type and F380Y channels, as indicated, recorded from inside-out macropatches. Voltage steps are from –80 to +80 mV in 20 mV increments and the internal [Ca^{2+}] is as indicated. Steady-state activation curves were obtained by converting ensemble (10 at each voltage) currents to conductance and fitting with a Boltzmann relation. Conductances of individual patches were normalized (G_{norm}) to the maximum conductance returned by the fit as described in the Methods and the plots for wild-type and F380Y channels are shown in *B*. The internal [Ca^{2+}] (μM) is as indicated next to each curve. A comparison of these plots shows that F380Y channels require much less Ca^{2+} to be active and are less voltage dependent than wild-type *hSlo*α channels. *C*, plot of $V_{1/2}$ values from the Boltzmann relations of *B* against [Ca^{2+}] for wild-type (●) and F380Y channels (○). *D*, mean–variance plots for wild-type (10 μM Ca^{2+}) and F380Y ('zero' Ca^{2+}) following pulses (83 for wild-type and 100 for F380Y) from –80 to +80 mV. The continuous lines show fits of these data to $\sigma^2 = iI - I^2/N$, where i = single channel current, I = total current and N = number of channels. For wild-type i = 31.9 pA and N = 329 corresponding to a maximum P_{open} of 0.861, and for F380Y i = 11.9 pA and N = 31, corresponding to a maximum P_{open} of 0.796. The data of F380Y do not begin at zero because of the steady-state activity present at –80 mV.

according to the following simplified scheme:

$$\text{Closed} \underset{k_c}{\overset{k_o}{\rightleftharpoons}} \text{Open}.$$

According to this scheme, relaxation time constants (activation or deactivation) and open probability are given, respectively, by:

$$\tau = 1/(k_o + k_c), \quad (2)$$

$$P_{open} = k_o/(k_o + k_c). \quad (3)$$

In these equations, k_o and k_c are the calculated opening and closing rate constants, and $k_o = k_o(0)\exp(-z_oFV/RT)$ and $k_c = k_c(0)\exp(-z_oFV/RT)$ where $k_o(0)$ and $k_c(0)$ are the values of k_o and k_c when $V = 0$ mV and z_o and z_c are the factors determining the voltage dependence of k_o and k_c, and F, R and T have their usual thermodynamic meanings. The relationship between membrane potential, relaxation time constants, and the steady-state activation curves were fitted simultaneously with eqns (2) and (3). The results of the fits are shown in Fig. 4*B* and the calculated opening and closing rate constants (k_o and k_c) for wild-type and F380Y channels in 10 μM Ca^{2+} are plotted against membrane potential in Fig. 4*C*. It is evident from Fig. 4*C* that a major effect on the gating of *hSlo*α channels of mutating F380 to Y is to decrease the closing rate constant, k_c, by more than an order of magnitude.

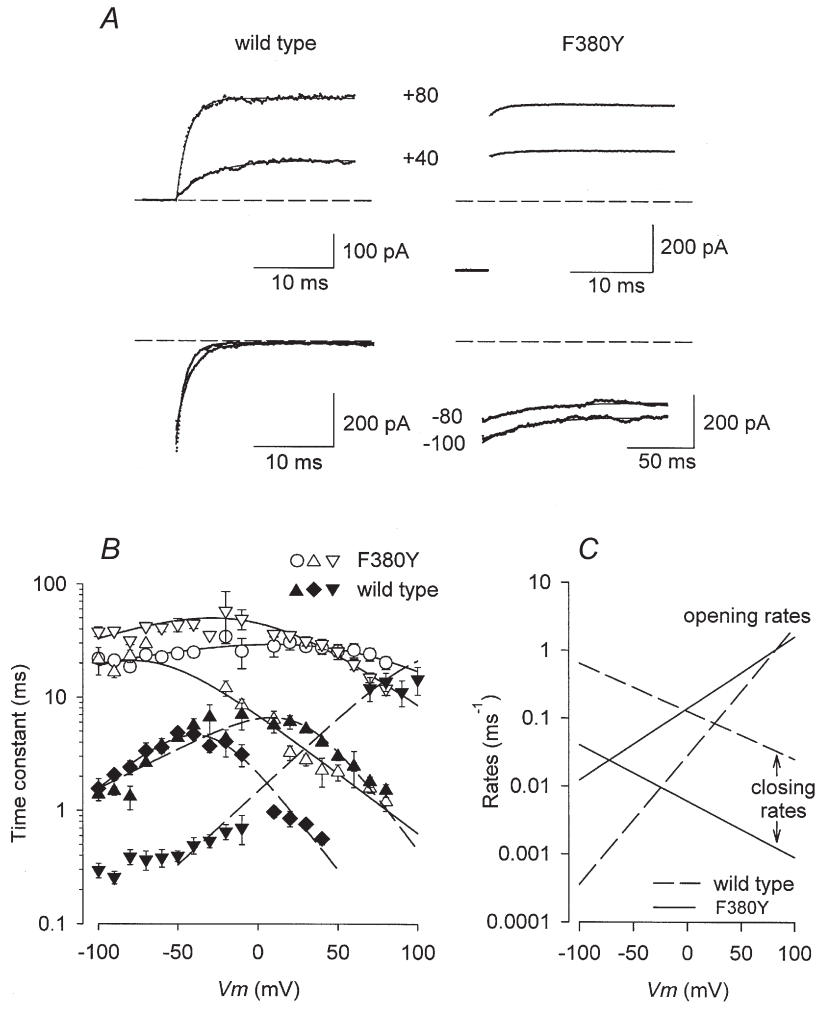

Figure 4. F380Y alters relaxation time course

A, currents (dotted trace) from wild-type and F380Y channels recorded at the potentials indicated and fitted (smooth lines) with an exponential function. The time course at negative potentials is much slower for F380Y than for wild-type currents (note difference in time scale). The dashed lines represent zero current. *B*, plots of the relaxation time constants (mean ± S.E.M.) measured at various potentials and [Ca^{2+}] for both wild-type (filled symbols) and F380Y (open symbols) currents. ○, 0 Ca^{2+}; ▼, ▽, 1 μM Ca^{2+}; ▲, △, 10 μM Ca^{2+}; ◆, 100 μM Ca^{2+}. The lines show the results of simultaneously fitting these data and those of the steady-state activation to eqns (2) and (3) as described in the text. *C*, plot of the opening and closing rate constants (k_o and k_c) as indicated for wild-type and F380Y channels in 10 μM Ca^{2+}.

DISCUSSION

A comparison of the sequence alignments of *hSloα* with those of other voltage-gated K^+ channels revealed that the equivalent residue to phenylalanine at position 380 in the S6 segment is isoleucine in *Shaker* and tyrosine in herg. We have analysed the effect of mutating this residue in *hSloα* to either Y (F380Y) or I (F380I) on unitary conductance, Ca^{2+} sensitivity and voltage-dependent gating.

Both F380Y and F380I channels were found to have a smaller single channel conductance than wild-type *hSloα*. This is consistent with the location of this residue being close to the inner mouth of the BK_{Ca} channel pore as predicted by the model of Doyle *et al* (1998). Tyrosine differs from phenylalanine only by the presence of a hydroxyl group, so it would be expected that this larger side chain interferes with ionic permeation. Such effects of altering side-chain size on unitary conductance have been studied in Kv2.1 by Liu & Joho (1998), who found that increasing the residue size increased conductance. In this study we found that mutating F380 to the smaller, but aliphatic, isoleucine gave a unitary slope conductance that was 31% of the wild-type channel. This suggests that the presence of an aromatic ring may be important in maintaining the high conductance of this channel by contributing to an electronegative environment in the intracellular vestibule.

Mutating this residue also had a dramatic effect on gating. Channels formed by F380I exhibited very low activity. Because of this, we were unable to obtain any additional information on the voltage and Ca^{2+} sensitivity of this mutant. In contrast, the currents produced by the mutation F380Y were large, and had a high open probability under all the conditions described. Distinct voltage-dependent currents were recorded with this mutant without requiring exposure to intracellular calcium. As calcium was reintroduced, activation required even less positive potentials until no significant rectification was observed in the voltage range studied. The Boltzmann distributions fitted to the F380Y data in Fig. 3 indicated that activation occurred at much more negative potentials, although the slope factors were not as steep as for the wild-type channel. These reduced slope factors result from a reduction in the voltage dependence of the opening rate of this mutant as shown in Fig. 4*C*. Relaxation rates at negative potentials were also slower than those of wild-type channels when compared under similar conditions. By adding a hydroxyl group to make residue 380 of each subunit polar, the channel remained Ca^{2+} dependent but was able to occupy the open state at much more negative potentials and with less intracellular Ca^{2+} than wild-type *hSloα*.

The results of mutating F380Y support the allosteric model of calcium-dependent activation, which requires voltage-dependent opening in the absence of calcium (Horrigan *et al.* 1999). Such properties have been studied in *mSlo* channels (Horrigan *et al.* 1999; Horrigan & Aldrich, 1999; Talukder & Aldrich, 2000) but require special voltage-clamp protocols, evoking voltage steps up to +300 mV. The voltage for half-maximal activation of the wild-type channel in zero calcium estimated from Horrigan *et al.* (1999) is around 200 mV, but by changing F380 to tyrosine, as described here, this is shifted to around 50 mV.

Christ *et al.* (1998), have studied the potential of injecting *Slo*-related cDNA into animal tissue as a therapeutic approach to relaxing smooth muscle. Should this approach be pursued further, then the hyperactive F380Y mutant may be of use by encoding a constitutively active channel, rather than simply increasing channel numbers. The F380I and F380Y mutants described in the present study have potential as dominant negative or positive tools, respectively.

In this paper, we have described mutations of a residue in the S6 transmembrane domain, distinct from regions that have been targeted previously, e.g. the 'Ca^{2+} bowl' (Schreiber & Salkoff, 1997), the S4 putative voltage sensor (Díaz *et al.* 1998), and the S4–S5 linker (Sullivan *et al.* 1997). Previous alterations in these regions have altered voltage and/or calcium sensitivity, but not as severely as the single conservative mutations of F380 described in this study. We therefore postulate that the intracellular region of S6 in *hSloα* may form part of the activation gate, as suggested by classical models (Armstrong, 1971; Hille, 1992), and is very sensitive to mutation, and possibly to changes in the local chemical environment.

Armstrong, C. M. (1971). Interaction of tetraethylammonium ion derivatives with the potassium channels of giant axons. *Journal of General Physiology* **58**, 413–437.

Blatz, A. L. & Magleby, K. L. (1984). Ion conductance and selectivity of single calcium-activated potassium channels in cultured rat muscle. *Journal of General Physiology* **84**, 1–23.

Christ, G. J., Rehman, J., Day, N., Salkoff, L., Valcic, M., Melman, A. & Geliebter, J. (1998). Intracorporal injection of *hSlo* cDNA in rats produces physiologically relevant alterations in penile function. *American Journal of Physiology* **275**, H600–608.

Díaz, L., Meera, P., Amigo, J., Stefani, E., Alvarez, O., Toro, L. & Latorre, R. (1998). Role of the S6 segment in a voltage-dependent calcium-sensitive potassium (*hSlo*) channel. *Journal of Biological Chemistry* **273**, 32430–32436.

DiChiara, T. J. & Reinhart, P. H. (1995). Distinct effects of Ca^{2+} and voltage on the activation and deactivation of cloned Ca^{2+}-activated K^+ channels. *Journal of Physiology* **489**, 403–418.

Doyle, D. A., Cabral, J. M., Pfuetzner, R. A., Kuo, A., Gulbis, J. M., Cohen, S. L., Chait, B. T. & MacKinnon, R. (1998). The structure of the potassium channel: Molecular basis of K^+ conduction and selectivity. *Science* **280**, 69–77.

Hamill, O. P., Marty, A., Neher, E., Sakmann, B. & Sigworth, F. J. (1981). Improved patch-clamp techniques for high-resolution current recording from cells and cell-free membrane patches. *Pflügers Archiv* **391**, 85–100.

Hille B. (1992). *Ionic Channel of Excitable Membranes*, 2nd edn. Sinauer, Sunderland, MA, USA.

Horrigan, F. T. & Aldrich, R. W. (1999). Allosteric voltge gating of potassium channels I: mSlo ionic currents in the absence of Ca^{2+}. *Journal of General Physiology* **144**, 277–304.

Horrigan, F. T., Cui, J. & Aldrich, R. W. (1999). Allosteric voltage gating of potassium channels I: mSlo channel gating charge movement in the absence of Ca^{2+}. *Journal of General Physiology* **144**, 305–336.

Lagrutta, A., Shen, K.-Z., Rivard, A., North, R. A. & Adelman, J. P. (1998). Aromatic residues affecting permeation and gating in dSlo channels. *Pflügers Archiv* **435**, 731–739.

Lippiat, J. D., Standen, N. B. & Davies, N. W. (1998). Block of cloned BK_{Ca} channels (rSlo) expressed in HEK 293 cells by N-methyl D-glucamine. *Pflügers Archiv* **436**, 810–812.

Liu, Y. & Joho, R. H. (1998). A side chain in S6 influences both open-state stability and ion permeation in a voltage-gated K^+ channel. *Pflügers Archiv* **435**, 654–661.

McManus, O. B. & Magleby, K. L. (1991). Accounting for the Ca^{2+}-dependent kinetics of single large-conductance Ca^{2+}-activated K^+ channels in rat skeletal muscle. *Journal of Physiology* **443**, 739–777.

Meera, P., Wallner, M., Song, M. & Toro, L. (1997). Large conductance voltage- and calcium-dependent K^+ channel, a distinct member of voltage-dependent ion channels with seven N-terminal transmembrane segments (S0-S6), an extracellular N terminus, and an intracellular (S9-S10) C terminus. *Proceedings of the National Academy of Sciences of the USA* **94**, 14066–14071.

Miller, C., Latorre, R. & Reisin, I. (1987). Coupling of voltage-dependent gating and Ba^{2+} block in the high-conductance Ca^{2+}-activated K^+ channel. *Journal of General Physiology* **90**, 427–449.

Ottolia, M., Babini, E., Gazzotti, P., Possani, L.D. & Prestipino, G. (1999). Reconstitution of a voltage and calcium dependent potassium channel from rat cerebellum. *Brain Research* **815**, 410–413.

Schreiber, M. & Salkoff, L. (1997) A novel calcium-sensing domain in the BK channel. *Biophysical Journal* **73**, 1355–1363.

Schreiber, M., Yuan, A. & Salkoff, L. (1999). Transplantable sites confer calcium sensitivity to BK channels. *Nature Neuroscience* **2**, 416–421.

Shen, K. Z., Lagrutta, A., Davies, N. W., Standen, N. B., Adelman, J. P. & North, R. A. (1994). Tetraethylammonium block of Slowpoke calcium-activated potassium channels expressed in Xenopus oocytes: evidence for tetrameric channel formation. *Pflügers Archiv* **426**, 440–450.

Sullivan, D. A., Holmqvist, M. H. & Levitan, I. B. (1997). Characterizataion of gating and peptide block of mSlo, a cloned calcium-dependent potassium channel. *Journal of Neurophysiology* **78**, 2937–2950.

Talkukder, G. & Aldrich, R. W. (2000). Complex voltage-dependent behaviour of single unliganded calcium-sensitive potassium channels. *Biophysical Journal* **78**, 761–772.

Wallner, M., Meera, P., Ottolia, M., Kaczorowski, G. J., Latorre, R., Garcia, M. L., Stefani E. & Toro, L. (1995). Characterization of and modulation by a beta-subunit of a human maxi KCa channel cloned from myometrium. *Receptors and Channels* **3**, 185–99.

Wei, A., Solaro, C., Lingle, C. & Salkoff, L. (1994). Calcium sensitivity of BK-type K_{Ca} channels determined by a separable domain. *Neuron* **13**, 671–681.

Acknowledgements

We thank Pfizer Central Research, The Biotechnology and Biological Sciences Research Council, and The Royal Society for support. We thank the following from Pfizer Central Research (Sandwich, Kent, UK): Dr Peter Stacey and Dr Stephen Phillips for the donation of the pcDNA6-*hSlo*α construct and advice on the molecular biology protocols, Dr Ian Harrow for assembling and interpreting sequencing data, and Paula Daniels for advice on transfecting HEK 293 cells and generating the stable clones.

Corresponding author

N. W. Davies: Department of Cell Physiology and Pharmacology, University of Leicester, University Road, Leicester LE1 9HN, UK.

Email: nwd@le.ac.uk